Planar MESFET Grid Oscillators Using Gate Feedback

Robert M. Weikle, II, *Member, IEEE*, Moonil Kim, *Student Member, IEEE*, Jonathan B. Hacker, *Student Member, IEEE*, Michael P. De Lisio, *Student Member, IEEE*, and David B. Rutledge, *Senior Member, IEEE*

***Abstract*—A new method for quasi-optically combining the output power of MESFET's is presented in which drain and source leads couple directly to the radiated field. The design consists of a planar grid of devices placed in a Fabry–Perot cavity. Capacitive feedback is provided to the gate. This is in contrast to previous MESFET grid designs where the radiated electric field was coupled to the drain and gate currents [12]. The new gate-feedback grids can oscillate at much higher frequencies than these previous grids. The oscillation frequency is dependent on the device characteristics, the resonator cavity, and is also a function of the symmetries of the grid. A transmission-line model for the grid is discussed and used to design two oscillator arrays. Experimental results are presented for oscillator grids operating at *X*-band and *Ku*-band. A 16-element grid has produced 335 mW of power at 11.6 GHz with a DC-to-RF conversion efficiency of 20%. This design was scaled to produce a 36-element grid oscillator with output power of 235 mW at 17 GHz. These results represent a significant improvement in the performance of planar grid oscillators which were previously limited to an operating frequency of 5 GHz and output power of 6 mW per device when using the same transistor. In addition, the planar configuration of the grid is very convenient for monolithic integration and is easily scalable to millimeter-wave frequencies.**

I. Introduction

IN RECENT years, power-combining schemes involving microwave and millimeter-wave solid-state sources have received much attention. The development of high-power, efficient and reliable sources is necessary to take advantage of the broader bandwidths and higher resolution imaging possible at millimeter-wave frequencies. High-power vacuum tubes are capable of producing better than 100 W at 100 GHz but the size, weight, and required high-voltage power supplies often limit their usefulness [1]. Solid-state technology can provide devices that operate in the millimeter-wave range, however, the power output from these devices is quite limited. IMPATT's can produce a few watts of CW power at 100 GHz while Gunn diodes are capable of producing about 100 mW. In addition, Gunn diodes and IMPATT's suffer from poor DC-to-RF efficiencies [2]. Better efficiencies can be realized with transistors. Pseudomorphic HEMT amplifiers have produced output powers of 57 mW at 94 GHz and power-added efficiencies of over 20% [3]. Heterojunction bipolar transistors also have the potential to provide high power at millimeter-wave frequencies without need for sub-micron lithography. An HBT with emitter area of 80 μm^2 has shown 15 dB of gain with an output power of 16 dBm at 35 GHz [4].

A variety of methods for combining the output powers of solid-state devices have been developed. A good review of these methods is given by Russell [5] for the microwave region and Chang and Sun for millimeter-wave frequencies [6]. Many of these techniques involve resonant microwave cavities or hybrids that are scaled for millimeter-wave operation. There are several disadvantages to this approach. The size of the cavities must be scaled according to wavelength making circuit fabrication more difficult. Waveguide losses also become more severe at millimeter-wave frequencies. In addition, a power-combiner based on resonant cavities or hybrid couplers can only accommodate a limited number of devices.

An attractive approach for overcoming the limitations of conventional waveguide and hybrid power-combiners is to combine the output powers of many devices in free-space. Mink suggested using an array of millimeter-wave devices placed in an optical resonator as a means of large-scale power-combining [7]. Because the power is combined in free-space, losses associated with waveguide walls and feed networks are eliminated. The power can be distributed over a large number of devices which is advantageous for high-power applications. In addition, synchronization or locking of the devices is accomplished with optical resonators which are easily realizable at millimeter-wave frequencies.

Several types of quasi-optical power-combiners have been reported in the literature. One design utilizes an array of packaged devices placed on a grid of metal bars [8], [9]. The metal bars provide an excellent heat sink which is necessary for low efficiency devices such as Gunn diodes. Another approach involves an array of weakly coupled patch antenna elements [10]. This method is similar to classic antenna arrays in which each individual patch is a free-running oscillator containing an active device. The patch elements are synchronized through the

Manuscript received August 29, 1991; revised February 20, 1992. This work was supported by the Army Research Office and the Northrop Corporation. J. B. Hacker holds an NSERC fellowship from Canada and M. P. De Lisio holds an NSF fellowship.

R. M. Weikle, II, is with the Department of Applied Electron Physics, Chalmers University of Technology, S412 96 Gothenburg, Sweden.

M. Kim, J. B. Hacker, M. P. De Lisio, and D. B. Rutledge are with the Division of Engineering and Applied Science, California Institute of Technology, Pasadena, CA 91125.

IEEE Log Number 9202891.

use of a partially transmitting reflector placed above the array. More recently, a two-sided microstrip configuration has been developed which permits isolation between an injection-locking signal and the array output [11]. A different design using a planar grid containing 100 packaged MESFET's in which all the devices lie in the same plane was developed by Popović *et al.* [12]. This grid produced an output power of 600 mW at 5 GHz with a DC-to-RF efficiency of 20%. The approach relies on the symmetries of the grid to provide the impedances necessary for oscillation to occur. The structure is similar to a laser oscillator in which the grid of MESFET's acts as a gain medium inside a Fabry–Perot cavity. An advantage of the planar configuration is its amenability to wafer-scale integration, which is necessary for scaling to millimeter-wave frequencies.

In this paper, we introduce a new planar grid configuration. The design permits higher frequency operation than possible with previous planar grid configurations. A simple transmission-line model is used for the design. Results for oscillator grids operating in the *X*-band and *Ku*-band are presented.

II. Grid Configuration

There are two important factors which determine the behavior of a quasi-optical array. The first is the choice of devices used in the grid. Gunn diodes and IMPATT's have the advantage of being two-terminal devices and are thus easily incorporated into a grid array. The low DC-to-RF efficiency, however, is a major drawback. In addition, Gunn diodes are inherently unstable and synchronization can prove difficult. Others have found it necessary to individually bias each device in the array to facilitate locking [10]. In contrast, transistors have a control terminal which is separate from the output terminals. This permits the devices in the grid to be more easily stabilized, allowing the oscillation to be controlled through an appropriately designed feedback network.

The second major factor determining the behavior of a quasi-optical array is the grid's physical configuration. The grid structure, together with the optical resonator, provides an embedding circuit in which the solid-state devices are placed. The oscillation frequency, output power, and efficiency of the grid depend on the impedances this embedding circuit presents at the device terminals. The planar MESFET grid configuration is shown in Fig. 1. The MESFET's are placed at each node in the grid and are represented by open circles. The details of how the transistor is connected to the grid depends on the physical layout of the device and several options are possible. The DC bias is fed along horizontal leads which extend across the grid in the x-direction. Adjacent rows of devices share bias lines. The radiating leads run in the y-direction and are connected to two terminals of the transistor. The third MESFET terminal is connected to the center bias line which runs along the row of devices.

Previous work with planar MESFET grids utilized packaged devices [12]. One cell of this grid is shown in Fig. 2(a). The use of packaged devices (Fujitsu FSC11LF) restricted the grid to a vertical drain-gate configuration. The disadvantage of this design is that the gate lead of the transistor radiates. As a result, the MESFET gate is always strongly coupled to the radiated field and this leads to oscillation at lower frequencies where the devices have high gain.

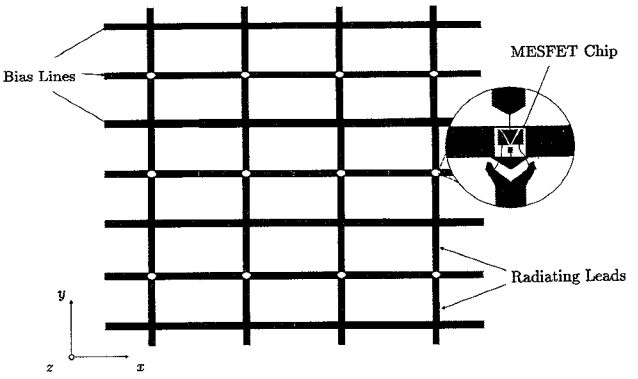

Fig. 1. Physical layout of the planar MESFET grid. MESFET's are represented as open circles and are placed at each node of the grid. Adjacent rows of devices share bias lines. The inset shows the detail of a transistor chip wire-bonded to the grid.

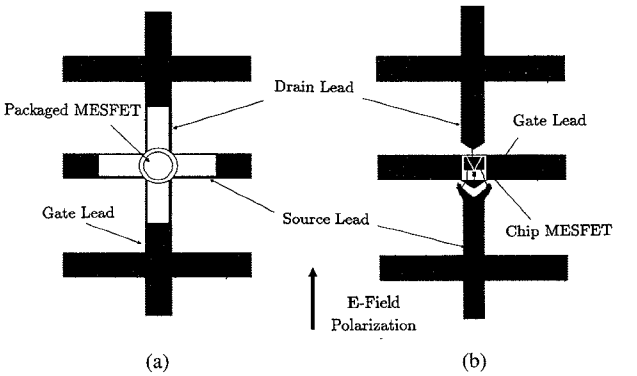

Fig. 2. (a) Unit cell for previous grid oscillators with packaged MESFET's. The drain and gate leads are parallel to the incident electric field. (b) Unit cell for the gate-feedback grid oscillator with chip MESFET's. The drain and source couple directly to the incident electric field. The gate leads, which run horizontally, are capacitively coupled to the incident field.

A configuration which overcomes this problem is shown in Fig. 2(b). Using a chip transistor the restrictions imposed by the package are eliminated and a vertical drain-source configuration can be realized. Bond wires are used to connect the device leads to the grid. The MESFET gate lead runs perpendicular to the radiated field and the feedback between the radiated field and gate now occurs through the MESFET embedding circuit.

III. Transmission-Line Model

To understand the behavior of a quasi-optical grid oscillator, it is necessary to know what impedances are present at the terminals of a MESFET placed in the array. The grid transmission-line model is based on an assumption that all devices in the grid are identical. For a grid infinite in extent, each transistor lies in an equivalent unit cell

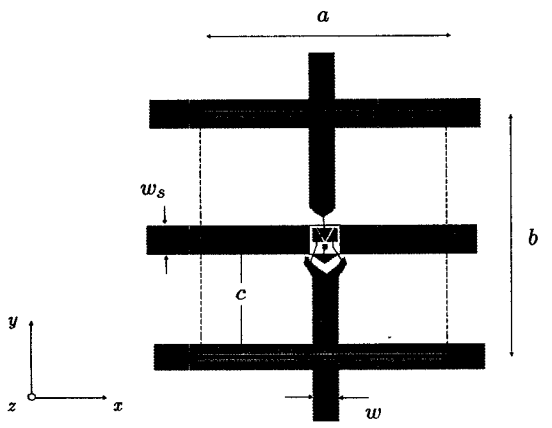

Fig. 3. Definition of the unit cell equivalent waveguide. The unit cell dimensions are indicated by the variables on the diagram. Electric walls are represented with solid lines and magnetic walls are represented with dashed lines.

which is defined by the grid symmetry. The field radiated by the infinite grid must satisfy symmetry-imposed boundary conditions at the unit cell edges as shown in Fig. 3. The unit cell is thus an equivalent waveguide representation for the entire grid. This equivalent waveguide has electric walls on the top and bottom and magnetic walls on the sides. It extends in the $+z$ and $-z$ directions, with the MESFET in the $z = 0$ plane. A transmission-line model representing the unit cell can be obtained using an EMF analysis similar to that of Eisenhart and Khan for a post in a waveguide [13]. The details of this analysis have been given elsewhere and it is not necessary to repeat them here [12].

The transmission-line model for the grid is shown in Fig. 4(a). The terminals labeled 1 and 2 represent connections to the vertical leads of the grid. The center terminal labeled 3 represents the horizontal lead. Currents in the vertical leads couple to the radiated field through a center-tapped transformer. Free space is modeled with a 377 Ω resistor which is scaled by the aspect ratio (b/a) of the unit cell. The mirror behind the grid is represented with a shunt short-circuited stub. The inductance of the radiating leads is shown as a series lumped inductor L. The horizontal leads do not couple directly to the radiated field but do produce evanescent modes which are modeled with a series capacitor and inductor (C_m and L_m). Expressions for the elements in the equivalent circuit model are derived from the EMF analysis and are given by

$$L = \frac{2b}{j\omega a} \sum_{\substack{m>0 \\ \text{m even}}}^{\infty} \operatorname{sinc}^2\left(\frac{m\pi w}{2a}\right) Z_{m0}^{\mathrm{TE}} \tag{1}$$

$$L_m = \frac{4}{j\omega ab} \sum_{\substack{m \text{ even} \\ m,n\neq 0}}^{\infty} \frac{1}{k_c^2} \sin^2\left(\frac{n\pi c}{b}\right) \operatorname{sinc}^2\left(\frac{m\pi w}{2a}\right) \cdot \operatorname{sinc}^2\left(\frac{n\pi w_s}{2b}\right) \left(\frac{k_x}{k_y} + \frac{k_y a}{k_x(a-w)}\right)^2 Z_{mn}^{\mathrm{TE}} \tag{2}$$

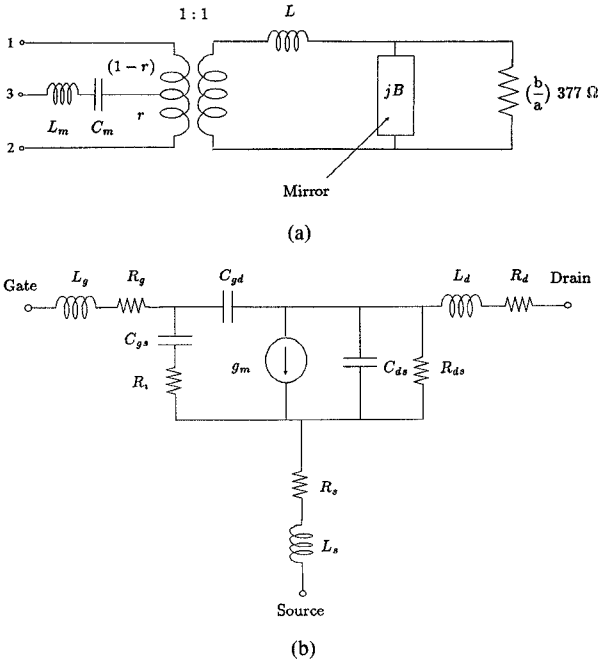

Fig. 4. (a) Transmission-line model for the planar MESFET grid. The transformer turns ratio is defined as $r = c/b$. (b) Equivalent circuit for the MESFET. The values for the lumped elements are obtained from the manufacturer's data sheet.

$$\frac{1}{C_m} = j\frac{2\omega}{ab}\left(\sum_{n=1}^{\infty} \frac{1}{k_y^2} \sin^2\left(\frac{n\pi c}{b}\right) \operatorname{sinc}^2\left(\frac{n\pi w_s}{2b}\right) Z_{0n}^{\mathrm{TM}} + 2 \sum_{\substack{m \text{ even} \\ m,n\neq 0}}^{\infty} \frac{1}{k_c^2} \sin^2\left(\frac{n\pi c}{b}\right) \operatorname{sinc}^2\left(\frac{n\pi w_s}{2b}\right) \cdot \operatorname{sinc}^2\left(\frac{m\pi w}{2a}\right) \left(1 - \frac{a}{a-w}\right)^2 Z_{mn}^{\mathrm{TM}}\right). \tag{3}$$

In the above expressions $k_x = m\pi/a$, $k_y = n\pi/b$, and $k_c^2 = k_x^2 + k_y^2$, where m and n are integers. Z_{mn}^{TE} and Z_{mn}^{TM} are the wave impedances for the mn-th TE and TM modes [14]. Each of these is a parallel combination of the impedances in the $+z$ and $-z$ directions.

The transmission-line model for the grid is completed by adding the equivalent circuit model for the MESFET. The model for the Fujitsu FSC11X is shown in Fig. 4(b). The values for the lumped elements in the model are provided by the manufacturer and depend on the transistor bias point. The complete circuit representing the vertical drain-source configuration of Fig. 2(b) is shown in Fig. 5. The drain and source of the MESFET are connected to terminals 1 and 2 of the transmission-line model. Because the grid embedding network provides a feedback path between the drain and gate, we refer to the vertical drain-source configuration as a "gate feedback" grid. The transconductance current of the MESFET is controlled by the voltage appearing across the gate-source capacitor. The loop gain of the circuit can be calculated using a test voltage with the current source and finding the resulting voltage induced across the gate-source capacitor. A loop gain

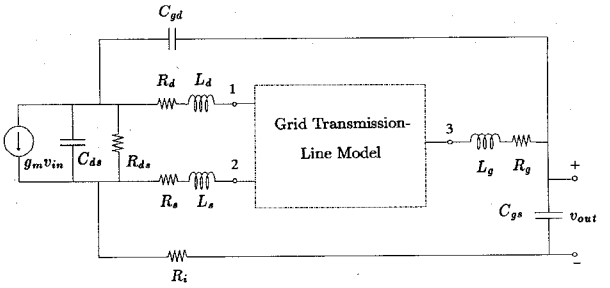

Fig. 5. Circuit model used to represent the planar grid with gate feedback. The grid embedding circuit of Fig. 4(a) is denoted by the dashed box. The voltage transfer function v_{out}/v_{in} is the loop gain of the system and is used to determine the frequency of oscillation.

of magnitude greater than unity with zero phase shift indicates an oscillation.

IV. *X*-Band MESFET Grid

A planar-grid oscillator may be designed using the appropriate device model in the circuit of Fig. 5. The dimensions of the grid as well as the substrate thickness and dielectric constant are parameters chosen to obtain oscillation at a desired frequency. An *X*-band grid oscillator designed from this circuit model is shown in Fig. 6. The grid contains 16 MESFET chips (Fujitsu FSC11X) spaced 9 mm apart in both the $\hat{x}$ and $\hat{y}$-directions. These devices, which have an f_T of 17 GHz and f_{max} of 33 GHz, are typically used for low-noise *C*-band amplifiers. The lead widths w and w_s are 1 mm and the substrate is 2.5 mm thick Roger's Duroid with $\epsilon_r = 2.2$. To preserve the symmetries assumed in the grid model, the vertical leads are extended a quarter wavelength above and below the array. This produces a low impedance where the unit cell is assumed to have an electric wall. Bond wires are used to bring the DC bias in to the horizontal leads. The inductance of these bond wires creates a high impedance on either side of the grid where a magnetic wall is needed to maintain symmetry. From the above dimensions, the radiating lead inductance, L, is calculated to be 3.4 nH. L_m and C_m are 0.94 nH and 304 fF, respectively.

A polar plot of the loop gain v_{out}/v_{in} for the grid is shown in Fig. 7. The loop gain has a magnitude of 2.7 and zero phase at a frequency of 11.67 GHz. Fig. 8 shows the spectrum measured in the far-field when the grid was biased with a drain voltage of 3 V and current of 200 mA. The effective radiated power (ERP) was measured at 15 W. For this measurement, a planar mirror was placed 14 mm behind the grid and a dielectric tuning slab was placed 2 cm in front of the grid. The dielectric slab (1.25 mm thick with $\epsilon_r = 10.2$) was found to be helpful in locking the grid to a single frequency, but not necessary. The mirror and dielectric slab can be used to tune the frequency and power of the oscillation. These tuning curves are shown in Fig. 9 for three different bias points. A theoretical frequency tuning curve obtained from the equivalent circuit model is shown for comparison and is within 2% of the measured curve. Gate bias voltage can also be used to tune the frequency but has little effect on the output

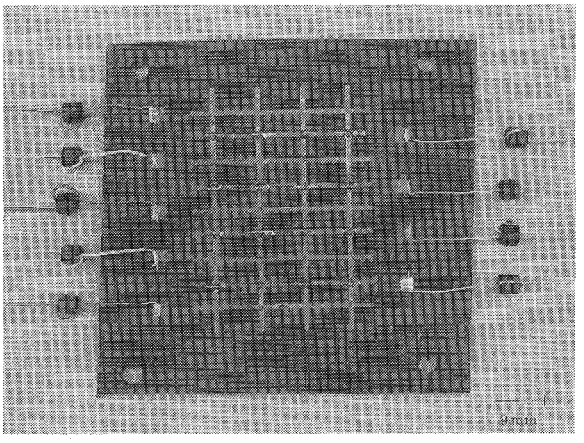

Fig. 6. Photograph of the *X*-band grid oscillator. The substrate is 2.5 mm thick Roger's Duroid with $\epsilon_r = 2.2$. The grid is placed between a mirror and dielectric slab which from the Fabry–Perot cavity. Ferrite beads are placed on the bias lines to suppress low-frequency oscillations.

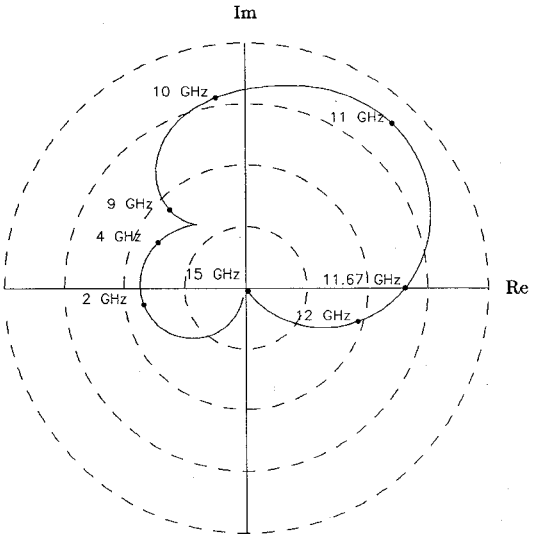

Fig. 7. Calculated loop gain of the *X*-band MESFET grid as frequency is swept from DC to 15 GHz. The locus crosses the zero-phase point at 11.67 GHz indicating an oscillation at that frequency.

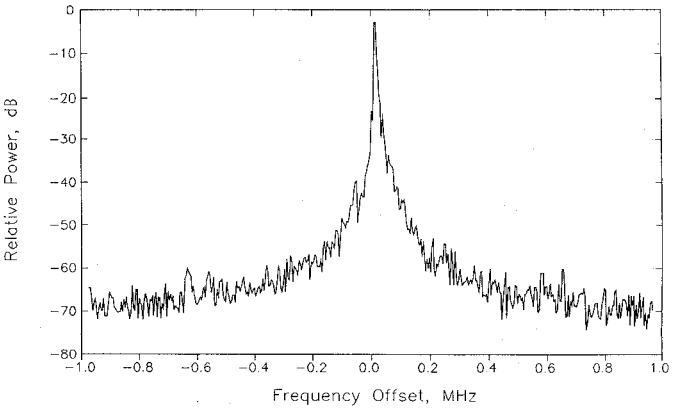

Fig. 8. Spectrum of the *X*-band MESFET grid. The center frequency is 11.58 GHz.

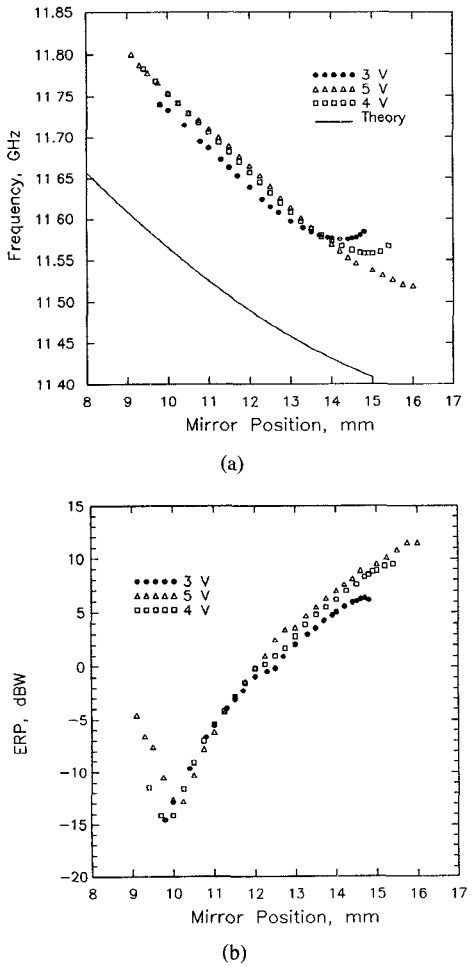

Fig. 9. (a) Oscillation frequency and (b) Power tuning of the grid as a function of mirror position for various drain biases. For these measurements a dielectric slab was placed 2 cm in front of the grid and the gate was biased at −1.4 V.

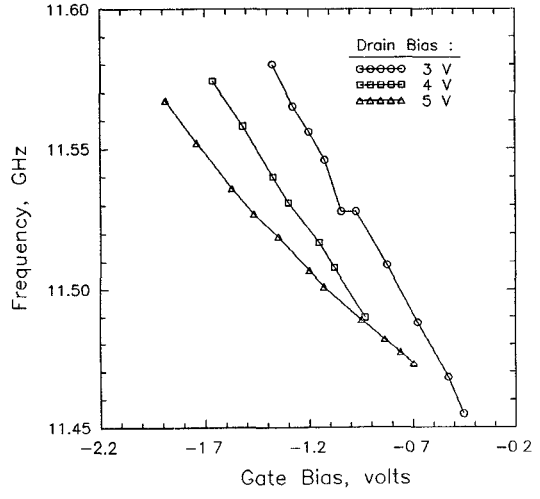

Fig. 10. Measured frequency tuning with gate bias voltage. The mirror was positioned 14 mm behind the grid with the dielectric slab 2 cm in front.

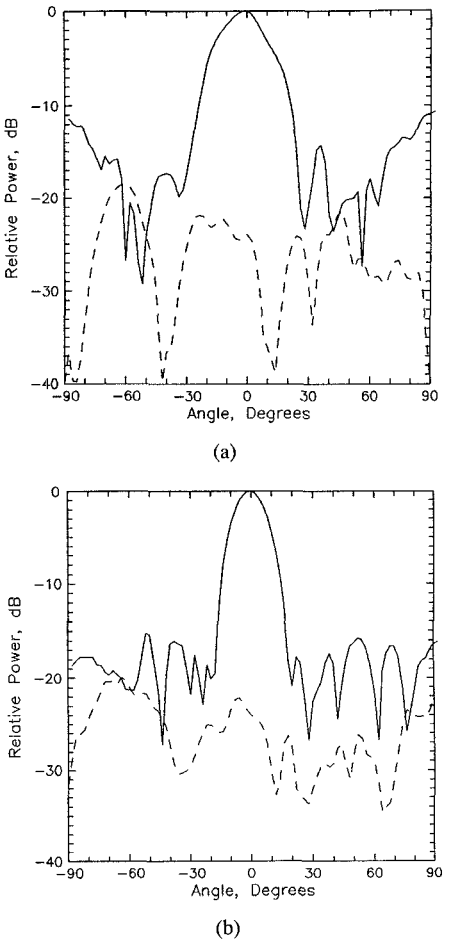

Fig. 11. Measured far-field radiation patterns from the *X*-band grid in the H-plane (a) and E-plane (b). The cross-polarized patterns are shown with the dashed lines.

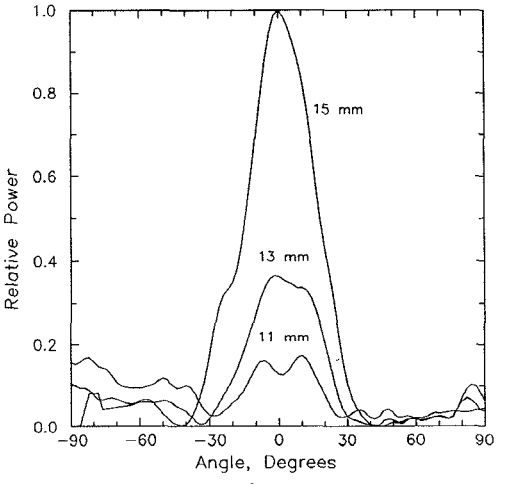

Fig. 12. Far-field H-plane pattern of the *X*-band grid as a function of mirror position. As the mirror is moved towards the grid the directivity and radiated power decrease.

power (Fig. 10). The far-field radiation pattern measured with a standard-gain pyramidal horn at a distance of 160 cm gave a maximum directivity of 16.5 dB (Fig. 11). The antenna pattern was also a strong function of mirror position as shown in Fig. 12. Maximum power radiated from the grid was measured to be 335 mW, or 20 mW per device. This corresponds to peak directivity and gave a DC-to-RF conversion efficiency of 20%.

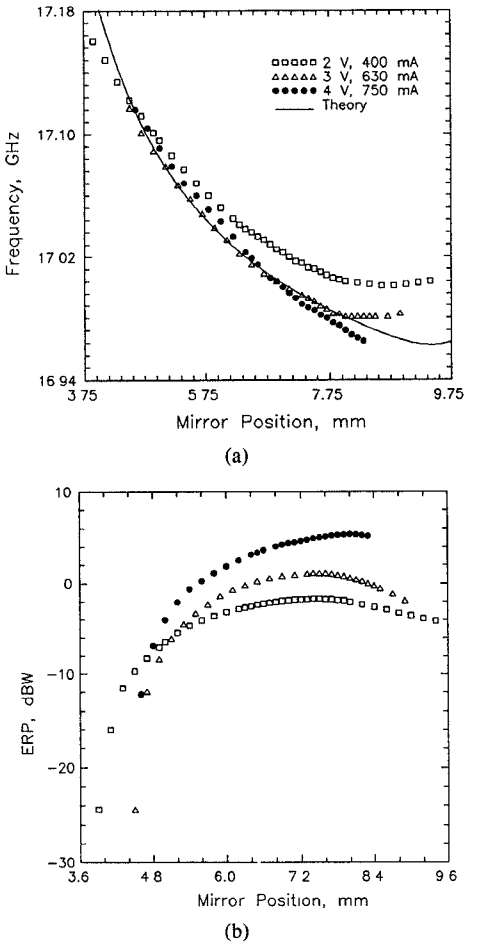

Fig. 13. Frequency (a) and power (b) tuning curves of the *Ku*-band MESFET grid for three different bias points. The measurements were taken without the front dielectric slab.

V. *Ku*-Band MESFET Grid

An advantage of the planar MESFET grid configuration is the ease with which it can be scaled for higher-frequency operation. Simulations with the equivalent circuit model indicate that oscillations near the f_T of the transistor are obtainable. The possibility of realizing an oscillator near 100 GHz with an appropriately designed grid of psuedomorphic HEMT's is quite attractive. To explore the feasibility of scaling grids to higher frequencies, the *X*-band grid oscillator previously discussed was scaled for operation in the *Ku*-band. The Ku-band design employed the same devices (FSC11X MESFET's) as the *X*-band oscillator. A 36-element grid was fabricated on a Duroid substrate (2.5 mm thick and $\epsilon_r = 2.2$) with a device spacing of 5 mm. The lead width was scaled to 0.5 mm and extended a quarter wavelength above the top row and below the bottom row of the grid.

Simulations performed with the equivalent circuit model indicated that the grid will oscillate at 17 GHz. Single frequency operation of the *Ku*-band grid was verified with a spectrum analyzer. As before, the power and frequency could be tuned with the backshort (Fig. 13). The grid produced an effective radiated power of 3.3 W which corresponds to a total radiated power of 235 mW. This is equivalent to 6.5 mW per device and gives a DC-to-RF conversion efficiency of 7%. The observed reduction in output power of the devices is expected due to the higher operating frequency. Typically, the power available from solid-state devices decreases with the inverse square of the frequency [15]. The measured far-field antenna patterns are shown in Fig. 14. The directivity of the grid was measured to be 11.5 dB.

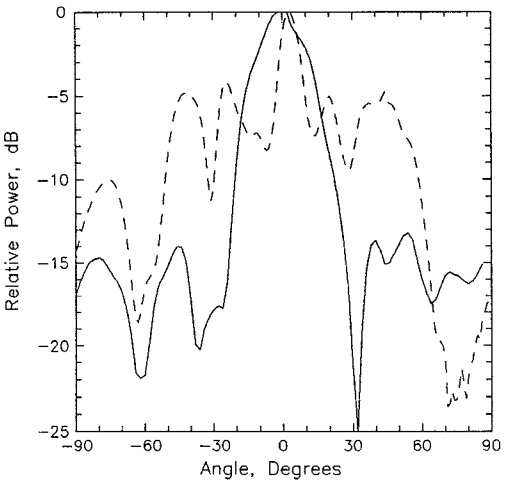

Fig. 14. Measured far-field patterns in the H-plane (———) and E-plane (- - -) for the *Ku*-band grid oscillator.

VI. Conclusions

A method for quasi-optical power combining with transistors has been described. The approach involves a planar periodic grid into which devices are embedded. A Fabry–Perot cavity is used to lock the devices to a single frequency which is determined by the resonator and the symmetry of the grid. The planar configuration is advantageous because it is simple and suitable for wafer-scale integration. A monolithically fabricated grid may potentially contain thousands of millimeter-wave devices for large-scale power combining. Use of a gate-feedback structure permits the grids to be operated at higher frequencies because the gate is not coupled directly to the radiated field. A transmission-line model used to predict the performance of the grid makes the design procedure straightforward. Grid oscillators are an attractive means of producing high-power radiation from solid-state sources and may be cascaded with other quasi-optical components such as grid mixers [16] and amplifiers [17] to produce a complete heterodyne receiver system.

References

[1] K. J. Sleger, R. H. Abrams, and R. K. Parker, "Trends in solid-state microwave and millimeter-wave technology," *IEEE Microwave Theory Tech. Newsletter*, no. 127, pp. 11–14, Fall 1990.

[2] T. B. Ramachandran, "Gallium arsenide power sources," *Microwave J.*, pp. 91–107, 1990 State of the Art Reference.

[3] P. M. Smith, P. C. Chao, J. M. Ballingall, and A. W. Swanson, "Microwave and mm-wave power amplification using pseudomorphic HEMTs," *Microwave J.*, pp. 71–85, May 1990.

[4] J. A. Higgins, "GaAs heterojunction bipolar transistors: A second

generation microwave power amplifier transistor," *Microwave J.*, pp. 176–194, May 1991.
[5] K. J. Russell, "Microwave power combining techniques," *IEEE Trans. Microwave Theory Tech.*, vol. MTT-27, pp. 472–478, May 1979.
[6] K. Chang and C. Sun, "Millimeter-wave power combining techniques," *IEEE Trans. Microwave Theory Tech.*, vol. MTT-31, pp. 91–107, Feb. 1983.
[7] J. W. Mink, "Quasi-optical power combining of solid-state millimeter-wave sources," *IEEE Trans. Microwave Theory Tech.*, vol. MTT-34, pp. 273–279, Feb. 1986.
[8] Z. B. Popović, R. M. Weikle, II, M. Kim, K. A. Potter, and D. B. Rutledge, "Bar-grid oscillators," *IEEE Trans. Microwave Theory Tech.*, vol. 38, pp. 225–230, Mar. 1990.
[9] M. Nakayama, M. Hieda, T. Tanaka, and K. Mizuno, "Millimeter and submillimeter wave quasi-optical oscillator with multi-elements," in *1990 IEEE MTT-S Int. Microwave Symp. Digest*, Dallas, May 1990, pp. 1209–1212.
[10] R. A. York and R. C. Compton, "Quasi-optical power combining using mutually synchronized oscillator arrays," *IEEE Trans. Microwave Theory Tech.*, vol. 39, pp. 1000–1009, June 1991.
[11] J. Birkeland and T. Itoh, "A 16-element quasi-optical FET oscillator power combining array with external injection locking," *IEEE Trans. Microwave Theory Tech.*, vol. 40, pp. 475–481, Mar. 1992.
[12] Z. B. Popović, R. M. Weikle, II, M. Kim, and D. B. Rutledge, "A 100-MESFET planar grid oscillator," *IEEE Trans. Microwave Theory Tech.*, vol. 39, pp. 193–200, Feb. 1991.
[13] R. L. Eisenhart and P. J. Khan, "Theoretical and experimental analysis of a waveguide mounting structure," *IEEE Trans. Microwave Theory Tech.*, vol. MTT-19, pp. 706–719, Aug. 1971.
[14] R. F. Harrington, *Time-Harmonic Electromagnetic Fields*. New York: McGraw-Hill, 1961, p. 152.
[15] S. M. Sze, *Physics of Semiconductor Devices, 2nd ed.* New York: Wiley, 1981, pp. 313–345.
[16] J. B. Hacker *et. al.*, "A 100-element planar schottky diode grid mixer," *IEEE Trans. Microwave Theory Tech.*, vol. 40, pp. 557–562, Mar. 1992.
[17] M. Kim *et al.*, "A grid amplifier," *IEEE Microwave Guided Wave Lett.*, vol. 1, pp. 322–324, Nov. 1991.

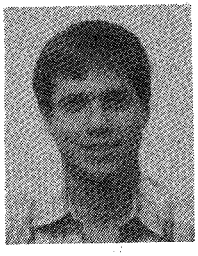

Robert M. Weikle, II (S'90–M'92) was born in Tacoma, WA on February 13, 1963. He received the B.S. degree in electrical engineering and physics from Rice University, Houston, TX, in 1986 and the M.S. and Ph.D. degrees from the California Institute of Technology, Pasadena, CA, in 1987 and 1992, respectively.

Currently, he is with the Department of Applied Electron Physics at Chalmers University of Technology in Göteborg, Sweden. His research interests include microwave and millimeter-wave solid-state devices, high-frequency circuit design, and quasi-optical components and techniques.

Moonil Kim (S'91) was born in Seoul, Korea on March 14, 1965. He received the B.S. degree from Illinois Institute of Technology in 1987, and the M.S. degree from California Institute of Technology in 1988. He is currently working toward his Ph.D. after joining the MMIC group at California Institute of Technology, where he is working on millimeter-wave beam steering circuitry.

Jonathan B. Hacker (S'84) was born in Vancouver, BC, Canada on February 16, 1963. He received the B.A.Sc. degree in electrical engineering in 1986 from the University of British Columbia, and the M.S. degree in electrical engineering from the California Institute of Technology, Pasadena in 1990. He is currently working towards the Ph.D. degree in electrical engineering at Caltech.

From 1986 to 1988 he was associated with the communications research and development group of the Nexus Engineering Corporation. His research interests include millimeter-wave quasi-optical techniques, microwave power amplifiers, and computer-aided design and measurement of microwave circuits.

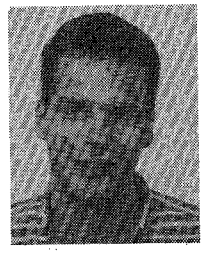

Michael P. De Lisio (S'90) was born in Detroit, MI, on July 29, 1968. He received the B.S.E. degree in electrical engineering from the University of Michigan, Ann Arbor, in 1990. In 1991, he obtained the M.S. degree from the California Institute of Technology.

Monolithic methods of millimeter-wave power combining and high-frequency solid-state devices are some of his research interests. He is currently pursuing the Ph.D. degree at the California Institute of Technology. Mr. De Lisio is a member of Tau Beta Pi and Eta Kappa Nu.

David B. Rutledge (S'75–M'80–SM'89) was born in Savannah, GA on January 12, 1952. He received the B.A. degree in mathematics from Williams College, Williamstown, MA in 1973, the M.A. degree in electrical sciences from Cambridge University, Cambridge, England, in 1975, and the Ph.D. degree from the University of California at Berkeley in 1980.

In 1980 he joined the faculty at the California Institute of Technology, Pasadena, CA, where he is now Professor of Electrical Engineering. His research is in developing millimeter and submillimeter-wave monolithic integrated circuits and applications, and in software for computer-aided design and measurement. He is co-author of the software CAD program, *Puff*, which has over 8000 users worldwide.